Friction and Wear Behavior of High-Silicon Lamellar Graphite Cast Iron Truck Brake Discs

Ali GÜNEN[*1] **ORCID** *0000-0002-4101-9520*
Melik ÇETİN[2] **ORCID** *0000-0002-6952-2523*
Tarkan SUBAŞ[3] **ORCID** *0009-0001-2395-9439*

[1]*Iskenderun Technical University, Faculty of Engineering and Natural Sciences, Metallurgical and Materials Engineering, Hatay, Türkiye.*
[2]*Karabük University, Faculty of Technology, Manufacturing Engineering, Karabük, Türkiye.*
[3]*Ekdöksan Döküm Metal Automotive San. Tic. Ltd. Şti., Konya, Türkiye*

Atıf şekli/ How to cite: GÜNEN, A., ÇETİN, M., SUBAŞ, T., (2023). Friction and Wear Behavior of High-Silicon Lamellar Graphite Cast Iron Truck Brake Discs. Cukurova University, Journal of the Faculty of Engineering, 38(4), 1023-1033.

Abstract

In this study, the chemical compositions of high-silicon lamellar graphite cast irons commonly used in truck brake discs and the effects of applied heat treatments on their friction and wear behaviors were investigated. For this purpose, samples with two different chemical compositions (first with 2.43 C and 4.5 Si; second with 2.5 C and 4.2 Si) were produced, and homogenization annealing was applied at 900°C for 30, 45, and 60 minutes followed by air cooling. Hardness, tensile testing, and wear testing were performed on the heat-treated samples. Wear tests were conducted at room temperature and dry sliding conditions (20 N load, 250 mm sliding distance, and 200 mm/min sliding speed) using a ball-on-disk wear apparatus against 52100 bearing steel. The increase in homogenization heat treatment time resulted in an increase in hardness and tensile strength values for both lamellar graphite cast iron grades. The wear test results indicated that both the chemical composition and the duration of applied heat treatment influenced the friction coefficient and wear volume losses. Since high friction coefficient and low wear volume losses are desired in brake discs, it was determined that the best result among the compared samples was achieved in the sample produced with a chemical composition of 2.5 C and 4.2 Si, and then homogenized at 900°C for 30 minutes.

Keywords: High-silicon lamellar graphite cast iron, Brake disc, Friction, Wear

Yüksek Silisli Lamel Grafit Dökme Demir Kamyon Fren Disklerinin Sürtünme ve Aşınma Davranışı

Öz

Bu çalışmada, kamyon fren disklerinde yaygın olarak kullanılan yüksek silisli lamelli grafitli dökme demirlerin kimyasal bileşimleri ve uygulanan ısıl işlemlerin sürtünme ve aşınma davranışları üzerindeki etkileri araştırılmıştır. Bu amaçla iki farklı kimyasal bileşime sahip (birincisi 2,5 C ve 4,2 Si; ikincisi 2,43

---

[*]Sorumlu yazar (Corresponding Author): Ali GÜNEN, *aligunen2013@gmail.com*

C ve 4,5 Si) numuneler üretilmiş ve 900°C'de 30, 45 ve 60 dakika homojenizasyon tavlaması ve ardından havada soğutma yapılmıştır. Isıl işlem görmüş numunelere sertlik, çekme testi ve aşınma testleri uygulandı. Aşınma testleri, oda sıcaklığında ve kuru kayma koşullarında (20 N yük, 250 mm kayma mesafesi ve 200 mm/dak kayma hızı) disk üzerinde bilyalı aşınma aparatı kullanılarak 52100 rulman çeliğine karşı gerçekleştirildi. Homojenizasyon ısıl işlem süresinin artması, her iki lamel grafitli dökme demir kalitesi için sertlik ve çekme mukavemeti değerlerinde artışa neden olmuştur. Aşınma testi sonuçları, hem kimyasal bileşimin hem de uygulanan ısıl işlem süresinin sürtünme katsayısını ve aşınma hacmi kayıplarını önemli ölçüde etkilediğini göstermiştir. Fren disklerinde yüksek sürtünme katsayısı ve düşük aşınma hacmi kayıpları istendiğinden, karşılaştırılan numuneler arasında en iyi sonucun 2,5 C ve 4,2 Si kimyasal bileşimi ile üretilip daha sonra 900°C'de 30 dakika süre ile homojenleştirilen numunede elde edildiği belirlendi.

Anahtar Kelimeler: Yüksek silisli grafitli dökme demir, Fren diski, Sürtünme, Aşınma

1. INTRODUCTION

Cast irons are alloys of Fe-C, where iron (Fe) is the primary constituent, and they may additionally incorporate other elements like carbon (C), silicon (Si), manganese (Mn), chromium (Cr), nickel (Ni), sulfur (S), phosphorus (P), and nitrogen (N). Within cast irons, there exist carbon crystals known as graphite. The microstructural characteristics of cast irons, including the shape and distribution of graphite, as well as the microstructure of the metal matrix, are contingent upon the chemical composition, casting procedure, and cooling circumstances [1-3]. Graphite is part of the microstructure of cast iron and according to this structure cast irons are classified into different types. Gray cast iron, white cast iron and ductile cast iron are classifications based on graphite structure. Gray cast irons have a lamellar graphite structure, white cast irons have a lamellar structure and ductile cast irons have a spherical graphite structure.

The shape of graphite in the structure is very important. Because the mechanical properties of cast irons vary depending on their chemical composition and graphite structure [4-6]. Although these alloys can be produced at low cost, the ability to achieve mechanical properties close to steels has made cast irons a popular material group used in a variety of industrial and engineering applications. Gray cast irons are used in a wide variety of applications. Examples include automobile engine parts, pipe fittings, construction materials, valves, pump housings, machine construction, brake linings and many other industrial and structural applications. Gray cast irons are low cost, well machinable, highly wear resistant and can be used in a variety of applications. However, cast irons also have some disadvantages, such as low strength and brittleness. Therefore, it is important to select the right type and apply appropriate heat treatments depending on the application requirements [2,3].

For this purpose, many studies have recently been carried out on the production of high silicon lamellar graphite cast irons. As the name suggests, this type of cast iron contains high amounts of silicon and lamellar (sheet-like) precipitated graphite [3]. Silicon is the alloying element that improves the mechanical properties of cast iron because it inhibits carbide formation and promotes graphite formation. It also improves wear resistance and provides resistance to oxidation. The lamellar precipitation of graphite gives lamellar graphite cast iron good vibration damping ability, high compressive strength [4-6], but also contributes to stress concentration and crack formation, thus affecting its mechanical properties [4]. The wear resistance of cast iron can be adversely affected by the undesirable characteristic resulting from the graphite morphology, particularly during dry sliding wear at high applied loads [7].

In the ferrite structure, silicon, one of the elements dissolved, enhances the hardness of ferritic gray cast iron [8]. The presence of silicon leads to an increase in the hardness of cast iron by promoting the formation of harder ferrite [8]. Nevertheless, silicon also induces the coarsening of graphite, causing a reduction in the hardness of cast iron [9]. An increase in ferrite formation corresponds to a

decrease in wear resistance, while enhanced graphite formation contributes to increased wear resistance [10]. This phenomenon involves the equilibrium between hardness attributed to ferrite influence and graphite influence, as well as the equilibrium between wear rates associated with ferrite and graphite influences.

While carbon is the most important element affecting the structure of cast irons, high levels of silicon also cause significant changes in the structure. In addition to increasing the fluidity of liquid cast iron, silicon has a significant effect on the carbon equivalent with C, and P. Based on the carbon equivalent ($CE = \%C + (\%Si + \%P) / 3$), this means that every 1% of silicon in the chemical composition will shift the eutectic point in the Fe-C equilibrium diagram of the alloy to the left by 0.3%. This means that cast iron compositions with a C content below 4.3% can solidify like a cast iron with a supra-eutectic composition. However, as the amount of silicon in the structure increases, the tensile strength of the cast iron decreases due to the decrease in the amount of austenite in the structure.

Although high silicon lamellar graphite cast iron can be produced with silicon in addition to iron and carbon, when cast irons used in industrial applications are examined, it can be seen that many different elements such as Cr, Mn and Cu are included in the structure besides these elements. There are reasons for adding these elements to the structure. Cr, being a strong carbide former, reduces the amount of graphite in the structure even when added in small amounts and may trigger freckle formation. Cu, on the other hand, in the range of 0.5-2.5% in liquid cast iron reduces freckle formation, while thinning the graphite structure and increasing its fluidity in the liquid state. However, if present in high proportions, Cu can cause embrittlement and especially edge cracks due to hydrogen sickness, which can cause major problems in casting. Mn, on the other hand, is not only a strong austenite former like Ni, but also an element that minimizes the negative effects of sulfur, as it enables sulfur, which causes brittleness in cast irons, to form the MnS compound primarily instead of FeS, so it is one of the elements that must be present in cast irons [11].

Due to the above-mentioned properties, high silicon lamellar graphite cast iron is a preferred material type, especially in heavy industry and engineering applications [12-15]. High silicon lamellar graphite cast irons are especially used in applications requiring high wear resistance [15]. Such cast irons are used in industrial pump parts, valve bodies, truck brake linings, medical devices and many other sectors. However, it is important to make sure that the grade and processing method chosen is suitable for the requirements of the application [13].

This investigation is centered on the application of high silica lamellar graphite cast irons in the manufacturing of truck brake discs. The rationale behind opting for high silica lamellar graphite cast irons lies in their multifaceted advantages, including notable wear resistance, a low coefficient of friction, high-temperature resilience, effective noise control, and the ease of casting [12,13]. In terms of wear resistance, the elevated silica content in these cast irons endows them with exceptional durability, thereby mitigating the wear and tear of brake discs subjected to friction and heat during wheel or disc brake application [14,15]. Additionally, the low coefficient of friction characteristic allows brake discs to smoothly interact with brake components, facilitating controlled braking for the driver. The high temperature resistance of high-silica lamellar graphite cast irons ensures the durability of brake discs under conditions of elevated temperatures during braking [16,17]. Addressing noise control concerns, this cast iron variety contributes to a quieter and more comfortable driving experience during brake disc utilization. Moreover, the ease of casting associated with high silica lamellar graphite cast irons enables the production of brake discs in diverse and intricate designs. Consequently, the utilization of high silica lamellar graphite cast irons in brake disc manufacturing emerges as a prevalent choice for ensuring the production of dependable and enduring brake system components. This material not only enhances brake performance but also contributes to the creation of long-lasting brake discs, thereby augmenting overall driving safety [14,15].

Ç.Ü. Müh. Fak. Dergisi, 38(4), Aralık 2023

1025

In this study, lamellar graphite cast iron specimens produced with two different chemical contents for use in brake linings were subjected to homogenization at 900°C for 30, 45 and 60 minutes and then air cooling processes. Considering brake lining applications, wear tests were carried out against a 6.3 mm diameter ball of 52100 bearing steel at 20 N load, 200 mm/sec speed and 250 m sliding distance.

2. EXPERIMENTAL METHODS

2.1. Materials

The samples of high-silicon lamellar graphite cast iron, with chemical compositions provided in Table 1, were melted in an induction furnace. After necessary chemical control and modification processes made, they were poured into sand molds prepared in the form of a molten metal brake disc model at 1390°C.

Table 1. %wt. chemical composition of high-silica content lamellar graphite cast irons (balance Fe)

Material	C	Si	Mn	Cu	Cr	S
D	2.43	4.5	0.49	0.19	0.27	0.066
T	2.5	4.2	0.5	0.2	0.26	0.068

In order to ensure the homogeneity of the samples produced by the sand mold casting method homogenization heat treatment was applied. The alloy containing 2.43 C 4.5 Si was annealed at 900°C for 30, 45 and 60 minutes and was not left to cool in the open air. These samples are coded as D1, D2 and D3, respectively. Similarly, the 2.5 C 4.2 Si alloy was annealed at 900°C for 30, 45 and 60 minutes and left to cool in open air. These samples are coded as T1, T2 and T3, respectively.

2.2. Applied Tests

After completing the heat treatment, specimens of appropriate dimensions for hardness measurements, tensile tests, and wear tests were extracted using a laser cutting machine. The surfaces of the specimens were then processed using a surface grinding machine. Subsequently, the surface roughness values of the specimens were measured using a 2D profilometer at a speed of 2 mm/s and a length of 4.8 mm. Hardness values were determined with a 1 kg load applied for 15 seconds. Tensile test specimens prepared according to the TSE EN ISO 6892-1 standard from the samples after heat treatment were subjected to tensile testing at a speed of 2 mm/min using a Shimadzu tensile testing machine with a capacity of 50 kN. The hardness values obtained and the tensile strength results from the experiments are presented in Table 2.

Table 2. Surface roughness, microhardness, and tensile strength of the samples before the wear process.

Sample	Surface roughness (μm)	Microhardness (HV)	Tensile strength (MPa)
D1	2.21	150	205
D2	2.75	170	270
D3	1.98	177	308
T1	2.66	220	307
T2	2.55	242	315
T3	2.50	255	340

Dry sliding wear tests were conducted on high-silicon lamellar graphite cast iron samples considering the wear conditions experienced by brake disc. The wear test parameters involved a computer-controlled ball-on-disk wear apparatus (Turkyus POD&HT&WT, Turkey) against a 52100 bearing steel ball with a diameter of 6.3 mm, a sliding speed of 200 mm/s, a load of 20 N, a wear track diameter of 7.7 mm, and a sliding distance of 250 m. The tests were carried out at room temperature under normal atmospheric conditions. During the wear test, friction coefficients (COF) were automatically recorded for each test using the computer interface of the wear apparatus. For each parameter, three repeated test data were averaged using an Excel program to create COF graphs.

The width and depth of the traces formed in the abrasion test were taken with a 2D profilometer and optical microscope, as the average of at least 4 traces on each sample, in the 0, 90, 270 and 360° parts of the circle. As can be seen from the optical profilometer images given in Section 3.1, the wear scar was evaluated to be in the shape of a half ellipse, and based on previous studies, the wear scar area was calculated with the following formulas.

1026

Ç.Ü. Müh. Fak. Dergisi, 38(4), Aralık 2023

The wear volume and wear rates were calculated as stated in Reference 18 using Excel and are given in Table 3.

$$L=2\pi r \tag{1}$$

$$V=0.25\pi WD \tag{2}$$

$$Wr=V/FS \tag{3}$$

Where L: Circumferential length of the wear scar (mm). V: Wear scar volume (mm3). r: Wear scar radius (mm) W: average wear scar width (μm). D: Average wear scar depth (μm). F: applied load (N). S: Sliding distance (m). and Wr: Wear rate (mm³/Nm).

3. RESULTS AND DISCUSSION

3.1. Friction Coefficient

The friction coefficient graphs of D1, D2 and D3 samples against 52100 bearing steel are given in Figure 1.
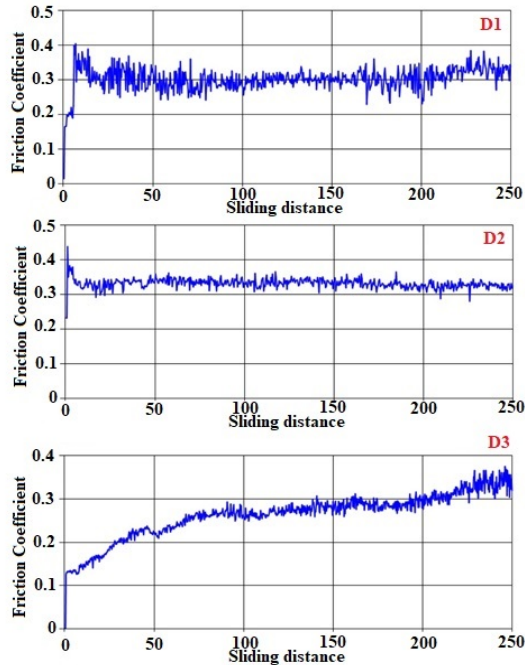
Figure 1. Friction coefficient graphs of samples D1, D2 and D3.

While the D1 and D2 samples maintained a stable friction coefficient around 0.3 throughout the test, it was observed that the D3 sample started at around 0.1 at the beginning of the test, followed a constantly increasing trend, and exceeded the 0.3 threshold at the end of the test. This shows that the homogeneity of sample D3 may be lower than other samples.
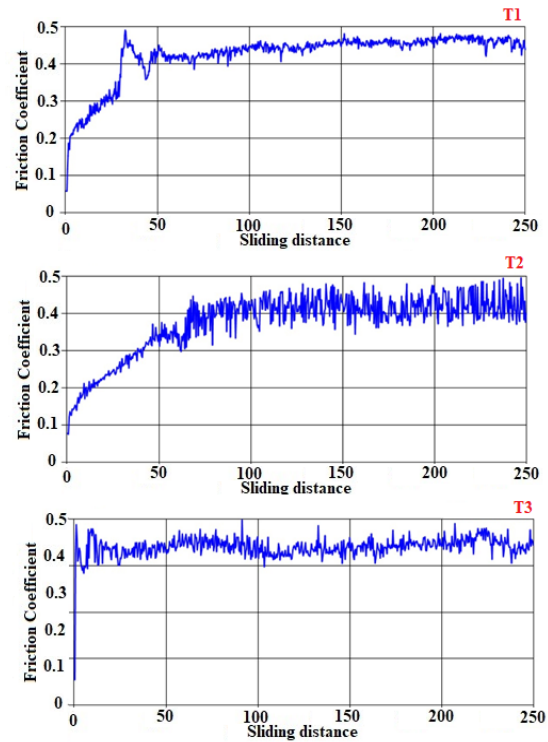
Figure 2. Friction coefficient graphs of samples T1, T2 and T3.

While the T1 and T2 samples started around 0.1 at the beginning of the test, reached a stable course of about 0.45 at the end of 50 m and continued in the range of 0.45-0.46 until the end of the test. On the other hand, the T3 sample followed a friction coefficient course in the range of 0.42-0.43 from the beginning to the end of the test. This is a result of the mechanical properties of T1 and T2 samples being close to each other. The fact that T3 showed more stable and a slightly lower coefficient of friction is a result of this sample having higher mechanical properties (hardness and tensile strength). As a matter of fact, the sample with

higher mechanical properties will show better resistance against the abrasive ball trying to sink into it, and the ball that does not sink into the substrate material will slide more easily [18,19].

Considering the graphs of the samples in Figure 1 and Figure 2 are compared with the studies in the literature, it can be seen that there is fluctuation in the friction coefficient of all the samples in this study. The situation of a continuous change with ups and downs has also been reported in studies in the literature [20-27]. Fluctuation in friction coefficient. It is related to the relationship between the deformation occurring during the test and the adhesive bond strength. Namely, the increasing trend of the friction coefficient is the result of the deformation occurring during the experiment and the adhesion of the abraded material to the surface. On the other hand, the decrease in the friction coefficient is the result of adhesive welding/bond breaking as the friction coefficient increases to high values. In their studies, Ping and his team [20] and Çetin et. al. [21] detected fluctuations in the friction coefficient during wear experiments and stated that this fluctuation was caused by the deformation that occurred during the experiment. They stated that graphite, which forms the matrix structure of cast iron, forms a graphite film on the wear surface. In this case, sliding does not occur regularly on the contacting surfaces and the formation of a film on the sliding surface of graphite does not prevent adhesive contact or adhesive bonding. However, they explained that it contributed to the bond being formed at a minimum level.

Anderson [22] describes this situation from a different perspective. He stated that it is caused by the formation of an oxide film on the surfaces that rub against each other during the wear process, due to the periodic and continuous change of temperature from the contact areas to the interior of the surfaces in contact during friction. It has been reported that a continuous change in the friction coefficient occurs due to the formation of the film and its breaking as a result of the acting forces. In another study reporting the fluctuation in friction coefficients [22], this situation was explained as welding of the asperities on the rubbing surfaces and the growth of these formations. The authors

reported that since the welding and separation process will be repeated continuously, an up-and-down graph will occur in the course of the friction coefficient. [20,23,24]. The continuous fluctuation of the friction coefficients measured in the wear tests was observed in both groups of lamellar graphite cast iron samples. It is thought that this is due to the microstructures not being homogeneous. Similar findings were reported by Jang et. al. [26] in their study on metal fiber brake discs. Because. Lamellar graphites have a lubricating effect, which indicates that the distribution of lamellar graphite's in gray cast iron can cause differences in the friction coefficient regime of the alloy. [9,10,26].

The behavior of materials under friction conditions is shaped depending on three main parameters [27]. These critical parameters are [21]:

1- Structure and surface properties: Factors such as the internal structure of the material, surface roughness, microstructure and chemical composition are the basic features that are effective in determining the friction behavior.
2- Friction type and test conditions: Factors such as the type of friction, that is, sliding or rolling, as well as the relative speed at which the experiment is carried out, the amount of load applied, the method of application and temperature, are other important parameters that affect the friction behavior.
3- Environmental conditions and lubrication: Conditions and lubrication surrounding friction have a significant effect on friction. Atmospheric conditions, humidity, degree of pollution and type of lubrication play an important role in determining friction behavior.

The combination of these factors requires a comprehensive evaluation to understand and optimize the friction performance of the material.

Additionally, as seen in Table 2, increasing the hardness of the samples resulted in a general decrease in the surface roughness values. However, it was determined that such a clear trend was not observed in the friction coefficients (Table 3). This

means that the friction coefficient is too complex to be associated only with hardness and surface roughness, and that it can vary depending on the interaction of many mechanical parameters of materials such as hardness, elastie modulus, fracture toughness [28]. Additionally, as the amount of silicone increased, the hardness increased, as can be seen in Table 2, and in parallel, there was a slight increase in the friction coefficient values (see Figure 1 and Figure 2). As a matter of fact, studies in the literature have reported that as the amount of silicon increases, the hardness values of gray/lamellar graphite cast iron decrease, but some increases occur in the friction coefficients [25,26].

3.2. Characterization of Wear Traces

Figure 3- Figure 8 shows the optical appearance and 2D profilometer images of the wear marks after the wear test.
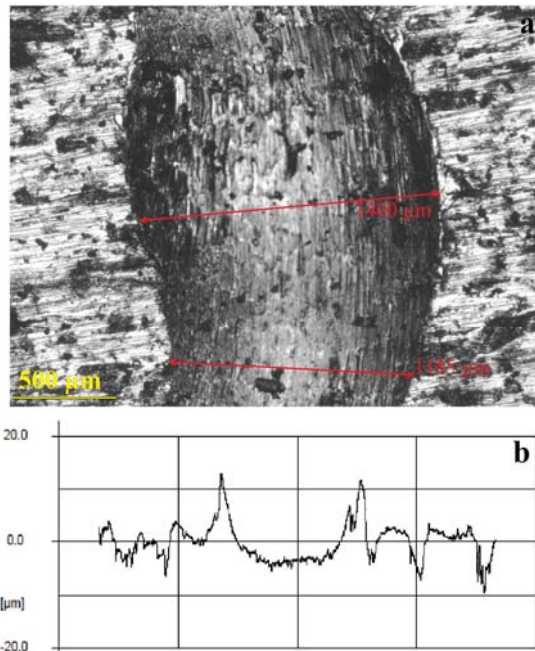
Figure 3. Illustration of wear scar width and depth of sample D1.

As Figure 3 is examined, it is noteworthy that there is some difference in the trace widths of the 3 samples taken from the D1 sample. This situation

can be attributed to the fact that the 30-minute homogenization anneal at 900°C applied to the D1 sample was insufficient. When the wear marks on the sample are examined, deep scratches, grooves and black areas are seen on the surface. This shows that the dominant wear mechanism in the sample is abrasive.
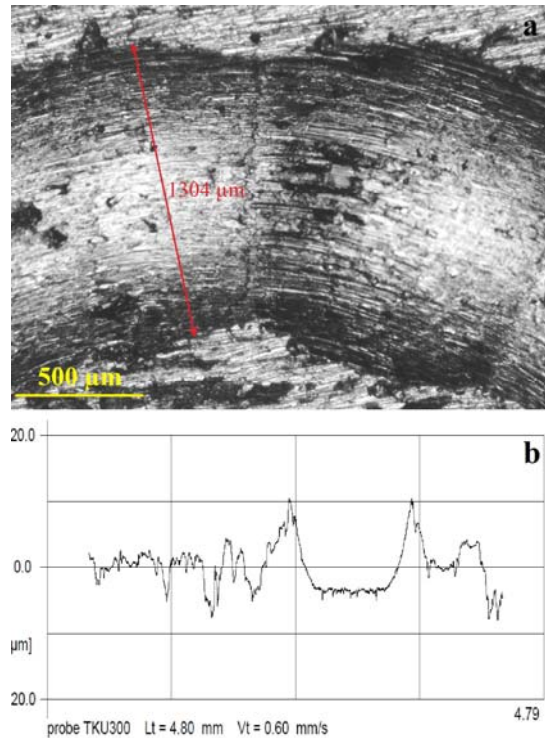
Figure 4. Illustration of wear scar width and depth of sample D2.

Whilst Figure 4 is inspected, although the trace widths taken from the D2 sample are similar to the D1 sample, they are closer to each other in the D2 sample. This shows that a 45-minute homogenization anneal at 900 °C minimizes the structural differences between the samples. This can be easily seen from the optical appearance of the wear marks on the sample. When the optical views are examined, it can be seen that the abrasive lines seen in the D1 sample are also seen in this sample, while the black areas that occur in the form of ruptures are not present.
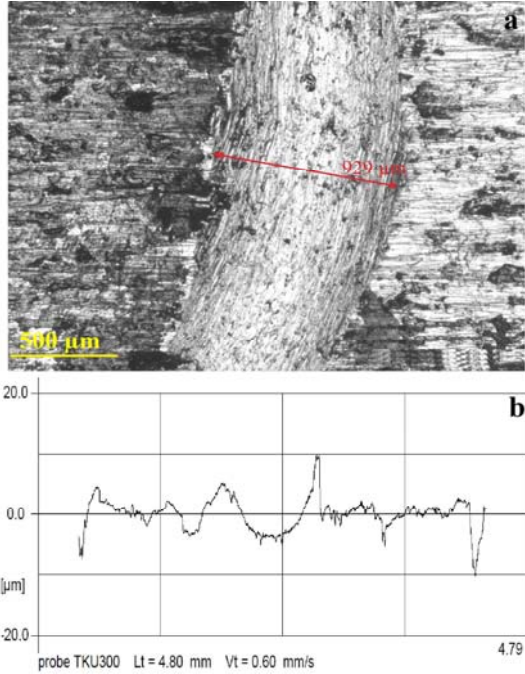
Figure 5. Illustration of wear scar width and depth of sample D3.

When Figure 5 is examined, it is seen that the wear scar width is quite low compared to D1 and D2 samples. This is a result of the D3 sample having a higher hardness value. Because. The high hardness of the material will better resist the plastic deformation of the ball trying to sink into it, depending on the applied load. However, if this hardness exceeds a certain degree, it will cause brittleness. As a matter of fact, when the worn surface optical images of the samples are examined, it is clearly seen that fractures (black areas) occur in places.

Once Figure 6 is assessed, it is determined that the trace widths of the 3 samples taken from the T1 sample is lower and shallower than the widths of the traces taken from the D1, D2, and D3 samples. This is a result of the high hardness values of the T1 sample in Table 2.

Figure 6. Illustration of wear scar width and depth of sample T1.
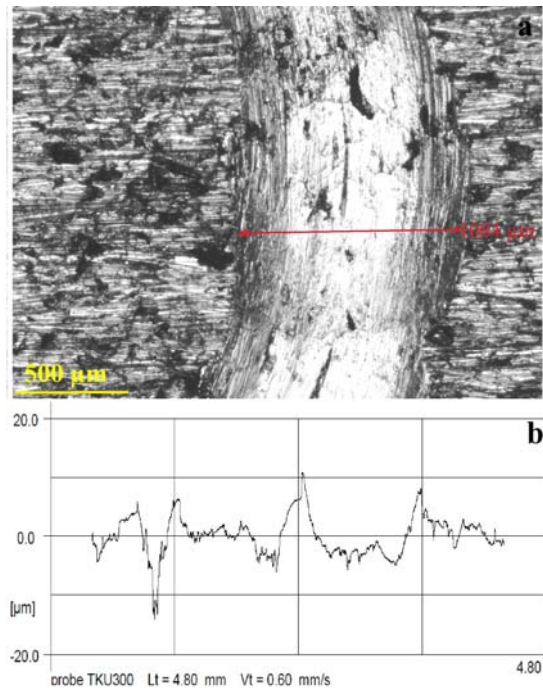
Figure 7. Illustration of the wear scar width and depth taken from the T2 sample.

Considering Figure 7, although values close to the wear scar widths taken on the T1 sample are obtained, the difference between the scars being

lower than T1 can be attributed to the fact that the 45-minute heat treatment period applied to the D1 samples obtained a more homogeneous structure compared to the 30-minute period. However, in the T2 sample, it is seen that the wear mechanism has evolved into fracture adhesive rather than abrasive.
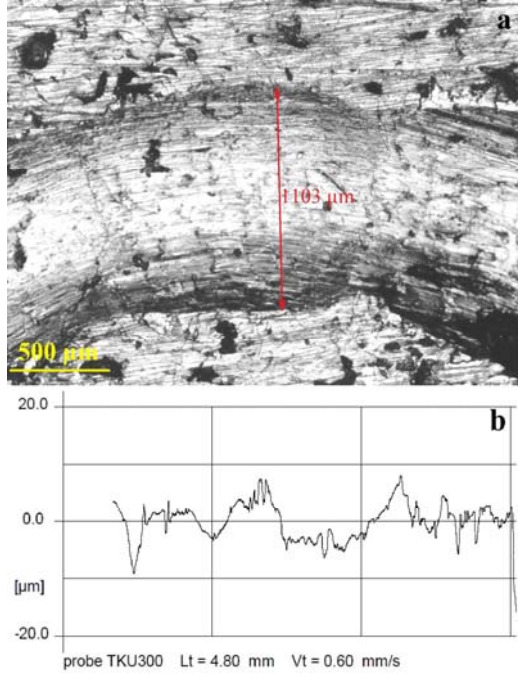
Figure 8. Illustration of the wear scar width and depth taken from the T3 sample.

As Figure 8 is examined, it can be seen that the wear scar widths taken from the T3 sample is wider than those of T1 and T2, but the wear scar depth is shallower. This may be due to the fact that the T3 sample has the highest hardness value, and therefore the abrasive ball, which does not sink into the sample easily, has worn out and created a larger contact area.

It is determined that the trace widths of the T samples (T1, T2 and T3) with higher Si content are lower and shallower than the widths of the traces taken from the D1, D2 and D3 samples. This is a result of the high hardness values of the T samples as seen in Table 2. Because samples with higher hardness values also have higher tensile stresses, they better resist the abrasive ball that tries to cause

plastic deformation on their surfaces. This results in less penetration of the ball into the material, resulting in lower wear scar width and depth. As a matter of fact, Table 3 supports this claim.

Table 3. Data obtained in wear test

Sample No	Mean COF	Wear scar width (µm)	Wear scar depth (µm)	Wear volume loss 10^{-2} (mm³)	Wear rate mm³/Nm
D1	0.304	1244.50	15	35.45	7.09
D2	0.331	1304.00	14	34.67	6.93
D3	0.262	926.33	10	17.59	3.52
T1	0.464	990.67	10	18.81	3.76
T2	0.438	1009.00	12	22.99	4.60
T3	0.424	1046.67	11	21.86	4.37

As seen in Table 3, as a result of the wear tests, the lowest friction coefficient value was obtained in the D3 sample as 0.262, while the highest friction coefficient value was obtained in the T1 sample with 0.464. on the other hand, the lowest wear volume loss occurred in the D3 sample and the highest wear volume loss occurred in the D1 sample.

4. CONCLUSION

In this study, the chemical contents of high-silica lamellar graphite cast iron produced for truck brake discs and the effects of applied heat treatments on friction and wear volume losses were examined. The results obtained can be briefly summarized as follows.

1- The increase in the duration of the homogenization process applied at 900 °C caused an increase in the hardness values and tensile strength values of the samples.
2- The applied heat treatment is more effective on the friction coefficient and wear volume rates of T1, T2 and T3 samples with lower Si content than D samples.

Ç.Ü. Müh. Fak. Dergisi, 38(4), Aralık 2023

1031

3- The lowest friction coefficient and wear volume loss occurred in the D3 sample heat treated at 900°C for 60 m.

4- While the wear volume losses of T samples are close to each other, the wear volume rates of D samples differ from each other. This situation reveals that the applied heat treatment is appropriate for T samples, but different parameters should be tested for D samples.

5- It has been concluded that the most suitable sample in brake disc selection among the compared samples is the T1 sample, as the desired brake discs are required to show a high coefficient of friction, enable stopping in shorter distances and have a longer life with lower wear and volume loss.

5. ACKNOWLEDGMENTS

6. AUTHORS' CONTRIBUTIONS

Ali GÜNEN and Melik Çetin designed the structure Tarkan SUBAŞ poured the sample according to the specifications. All authors carried out the experimental studies and the theoretical calculations and wrote up the article in collaboration. Ali GÜNEN and Melik ÇETİN are the overall supervisor of the project. All authors read and approved the final manuscript.

7. REFERENCES

1. Ertuğrul, O., Güzelipek, O., Soyusinmez, T., Akdoğan, A.T., Güneş, A.B., 2020. Dökme Demir Malzemelerin Karbür Uçlarla Delme İşleminde Proses Parametrelerinin Optimizasyonu, Çukurova Üniversitesi Mühendislik-Mimarlık Fakültesi Dergisi, 35(1), 251-262.

2. Collini, L., Nicoletto, G., Konečná, R.J.M.S., 2008. Microstructure and Mechanical Properties of Pearlitic Gray Cast Iron, Materials Science and Engineering: A, 488(1-2), 529-539.

3. Herring, D.H., Heat Treatment of Cast Iron. https://industrialheating.com/articles/94644-heat-treatment-of-cast-irons, Access date: 12.05.2023

4. Agunsoye, J.O., Isaac, T.S., Awe, O.I., Onwuegbuzie, A.T., 2013. Effect of Silicon Additions on the Wear Properties of Grey Cast Iron. Journal of Minerals and Materials Characterization and Engineering, 1, 61-67.

5. Angus, H.T., 2013. Cast Iron: Physical and Engineering Properties. Elsevier, 542.

6. Davis, J.R., (Ed.). 1996. ASM Specialty Handbook: Cast Irons. ASM International, 494.

7. Mohamadzadeh, H., Saghafian, H., Kheirandish, S., 2009. Sliding Wear Behavior of a Grey Cast Iron Surface Remelted by TIG. Journal of Materials Science and Technology, 25(5), 622-628.

8. Singh, V., 1999. Physical Metallurgy. (1st ed.) Delhi: Globe Offset Press Chapter 11, 608-609.

9. Darmo, S., Setyana, L.D., Tarmono, T., Santoso, N., 2018. The Effects of Silicon on the Hardness and Wear of Ferritic Grey Cast Iron on Shoe Brake of Train. In IOP Conference Series: Materials Science and Engineering, 384(1), 012017, IOP Publishing.

10. Singhal, P., Saxena, K.K., 2020. Effect of Silicon Addition on Microstructure and Mechanical Properties of Grey Cast Iron: An Overview, Materials Today: Proceedings, 26, 1393-1401.

11. Ünal, E., Yaşar, A., Karahan, İ.H., 2021. Elektrokimyasal Depolama Yöntemi ile AISI 304 Çeliği Yüzeyine Biriktirilen Ni-B/TiB$_2$ Kompozit Kaplamaların Kristal Yapı ve Bazı Mekanik Özelliklerinin İncelenmesi. Çukurova Üniversitesi Mühendislik Fakültesi Dergisi, 36(4), 847-860.

12. Stoian, E.V., Bratu, V., Enescu, C.M., Ungureanu, D.N., 2018. Researches Regarding the Influence of Alloying Elements on the Mechanical Properties of Lamellar Graphite Cast Iron, Scientific Bulletin of 'Valahia' University. Materials and Mechanics, 16(15), 11-16.

13. Stefanescu, D.M., 2017. Classification and Basic Types of Cast Iron, ASM International.

14. Riposan, I., Stan, S., Anca, D., Stefan, E., Stan, I., Chisamera, M., 2023. Structure

Characteristics of High Si Ductile Cast Irons. International Journal of Metal Casting, 1-24.

15. Ghasemi, R., 2016. The Influence of Microstructure on Mechanical and Tribological Properties of Lamellar and Compacted Irons in Engine Applications. Doctoral Dissertation, Jönköping University, School of Engineering, Jönköping, 94.

16. Wang, G.Q., Liu, Z.L., Li, Y.X., Chen, X., 2022. Different Thermal Fatigue Behaviors between Gray Cast Iron and Vermicular Graphite Cast Iron. China Foundry, 19(3), 245-252.

17. Elliott, R., 1988. Cast Iron Technology. Butterworths, Elsevier Science London, 847.

18. Gunen, A., Ulutan, M., Gok, M.S., Kurt, B., Orhan, N., 2014. Friction and Wear Behavior of Borided AISI 304 Stainless Steel with Nano Particle and Micro Particle Size of Boriding Agents. Journal of the Balkan Tribological Association, 20(3), 362-379.

19. ELSawy, E., El-Hebeary, M.R., El Mahallawi, I.S.E., 2017. Effect of Manganese Silicon and Chromium Additions on Microstructure and Wear Characteristics of Grey Cast Iron for Sugar Industries Applications. Wear, 390, 113-124.

20. Ping, L., Bahadur, S., Verhoeven, J.D., 1990. Friction and Wear Behavior of High Silicon Bainitic Structures in Austempered Cast Iron and Steel. Wear, 138(1-2), 269-284.

21. Çetin, M., Gül, F., 2007. Kuru Kayma Şartlarında Matris Yapısının Küresel Grafitli Dökme Demirin Sürtünme Katsayısına ve Pim Sıcaklığına Etkisi. Gazi Üniversitesi Mühendislik Mimarlık Fakültesi Dergisi, 22(3). 273-280.

22. Anderson, A.E.,1992. Friction, Lubrication and Wear Technology. ASM Handbook, 8, 569-577.

23. Stachowiak, G., Batchelor, A.W., 2013. Engineering Tribology. Elsevier, 871.

24. Jacuinde, A.B., Rainforth, W.M., 2001. The Wear Behaviour of High-chromium White Cast Irons as a Function of Silicon and Mischmetal Content. Wear, 250(1-12), 449-461.

25. Catalán, N., Ramos-Moore, E., Boccardo, A., Celentano, D., 2022. Surface Laser Treatment of Cast Irons: A Review. Metals, 12(4), 562.

26. Jang, H., Ko, K., 2004. The Effect of Metal Fibers on the Friction Performance of Automotive Brake Friction Materials. Wear, 256, 406-414.

27. Tonghe, Z., Huixing, Z., Ji, H., Xiaoji Yuguang, W., Furong, M., Hong, L., Hanzhang, S., Jianzhong, S., 2000. Industrialization of Mevva Source Ion Implantation. Surface and Coatings Technology, 128-129, 1-8.

28. Günen, A., Kurt, B., Milner, P., Gök, M.S., 2019. Properties and Tribological Performance of Ceramic-base Chromium and Vanadium Carbide Composite Coatings. International Journal of Refractory Metals and Hard Materials, 81, 333-344.

Ç.Ü. Müh. Fak. Dergisi, 38(4), Aralık 2023

1033

1034

Ç.Ü. Müh. Fak. Dergisi, 38(4), Aralık 2023